Resonance-like production of tensor polarization in the interaction of an unpolarized deuteron beam with graphite targets

To cite this article: H Seyfarth *et al* 2011 *J. Phys.: Conf. Ser.* **295** 012125

View the article online for updates and enhancements.

Resonance-like production of tensor polarization in the interaction of an unpolarized deuteron beam with graphite targets

H Seyfarth[1], V Baryshevsky[2], C Düweke[3,a], R Emmerich[3,b], R Engels[1], K Grigoryev[1,4], A Imig[3,c], M Mikirtychiants[1,4], F Rathmann[1], A Rouba[2], H Ströher[1] and A Vasilyev[4]

[1]Institut für Kernphysik, Jülich Center for Hadron Physics, Forschungszentrum Jülich, 52425 Jülich, Germany
[2]Research Institute for Nuclear Problems, Bobruiskaya ul. 11, 220050 Minsk, Belarus
[3]Institut für Kernphysik, Universität zu Köln, Zülpicher Straße 77, 50937 Köln, Germany
[4]Petersburg Nuclear Physics Institute, 188300 Gatchina, Russia

E-mail: H.Seyfarth@fz-juelich.de

Abstract. As shown in a recent paper, an initially unpolarized beam of deuterons can acquire appreciable tensor polarization by traversing a graphite foil. Here those results are presented which result when the earlier linear fits to the measured data are replaced by quadratic fits, taking into account slight non-linearities. The parameters of the fit to the energy dependence of the tensor polarization are discussed. Measured asymmetries confirm the azimuthal symmetry of the beam behind the targets. The values of p_{zz}, achievable with graphite foils, are discussed.

1. Introduction

Nuclear spin dichroism leads to the appearance of tensor polarization in an initially unpolarized, forward-transmitted beam of (spin 1) deuterons behind a target composed of spin-zero nuclei like carbon [1]. The direction of the primary and the transmitted beam defines the quantization axis. Because of the azimuthal symmetry, the polarization of the beam behind the target is described by the tensor-polarization component p_{zz}. In the unpolarized initial beam of total intensity $I_{\text{tot}}(0)$, the relative intensities of deuterons in the substates $m = +1$, $m = 0$ and $m = -1$ are $I_{+1}(0) = I_0(0) = I_{-1}(0) = \frac{1}{3}I_{\text{tot}}(0)$. Due to its definition (e.g., [2]) $p_{zz}(0) = (I_{\text{tot}}(0) - 3I_0(0))/I_{\text{tot}} = (I_{+1}(0) + I_{-1}(0) - 2I_0(0))/I_{\text{tot}}(0)$ is equal to 0. Accordingly, p_{zz} behind the target reads

$$p_{zz}(\rho d) = \frac{I_{+1}(\rho d) + I_{-1}(\rho d) - 2I_0(\rho d)}{I_{+1}(\rho d) + I_{-1}(\rho d) + I_0(\rho d)}, \tag{1}$$

where ρ is the number density of nuclei in the target (per unit of volume) and d its thickness (in units of length). The interaction of deuterons of energy E with the spin-zero target nuclei is described by total cross sections σ_{+1}, σ_{-1} and σ_0. The symmetry in the interaction allows to set $\sigma_{+1} = \sigma_{-1} = \sigma_{\pm1}$. For a thin target of thickness δ and negligible energy loss of the deuterons,

$I_{+1}(\rho\delta) = I_{-1}(\rho\delta) = \frac{1}{3}exp[-\sigma_{\pm 1}(E)\delta]$ and $I_0(\rho\delta) = \frac{1}{3}exp[-\sigma_0(E)\delta]$. For a thick target, p_{zz} results from integration over the range of deuteron energies in the target as

$$p_{zz}(\rho d) = \frac{2e^{-\rho \int_0^d \sigma_{\pm 1}(E(x))dx} - 2e^{-\rho \int_0^d \sigma_0(E(x))dx}}{2e^{-\rho \int_0^d \sigma_{\pm 1}(E(x))dx} + e^{-\rho \int_0^d \sigma_0(E(x))dx}}. \tag{2}$$

The integrals cover the cross section values between those at the initial beam energy, $\sigma_{\pm 1,0}(E_{in}(x=0))$, and those at the beam energy behind the target, $\sigma_{\pm 1,0}(E_{out}(x=d))$.

Measurements of p_{zz}, produced by a set of graphite targets, have been performed with unpolarized deuteron beams from the HVEC FN Van de Graaf tandem accelerator of the Institut für Kernphysik of the Universität zu Köln. The experimental setup with the polarimeter, based on the $\vec{d} + {}^3\text{He} \rightarrow p + {}^4\text{He}$ reaction, was described in a recent paper [3]. The values of p_{zz} were derived from linear fits to the ratios of counts in the five proton detectors of the polarimeter, measured as function of the deuteron energy in the polarimeter cell. The results of the present contribution were obtained by replacing the earlier linear fit functions by quadratic functions to account for slight non-linearities.

2. Experimental procedure and results

As discussed in Ref. [3], for each of the seven graphite targets and the gold reference target a set of primary beam energies E_{in} with steps of 0.1 MeV was utilized, chosen such that the deuteron energies E_c in the ${}^3\text{He}$ gas cell of the polarimeter ranged from 5 to 8 MeV (see table 1). The

Table 1. Target material M and areal density d_t, target label, run (I: 2003, II: 2006), minimal and maximal primary deuteron beam energies E_{in}, and minimal and maximal mean deuteron energies E_c in the ${}^3\text{He}$ polarimeter cell.

M	d_t [mg/cm^2]			Label	Run	E_{in} [MeV]		E_c [MeV]	
						min	max	min	max
Au	5.0	$\pm$	0.3	Au5	II	6.20	7.90	5.56	7.36
C	35.90	$\pm$	0.19	C36	II	9.50	10.50	6.06	7.41
C	57.69	$\pm$	0.32	C58	I	10.80	12.20	5.73	7.83
C	93.59	$\pm$	0.37	C94	II	13.00	14.00	5.72	7.46
C	129.49	$\pm$	0.42	C129	II	14.80	15.90	5.41	7.55
C	152.63	$\pm$	0.75	C153	I	16.20	16.70	5.94	6.97
C	165.39	$\pm$	0.46	C165	II	16.70	17.50	5.70	7.39
C	187.93	$\pm$	0.74	C188	I	17.50	18.70	5.11	7.78

tensor polarization of the beam behind a target for a value of E_c is derived from the ratio

$$r(E_c) = \frac{N_L(E_c) + N_U(E_c) + N_R(E_c) + N_D(E_c)}{N_F(E_c)}. \tag{3}$$

The $N_i(E_c)$ denote the counts of protons from the polarimeter reaction in the four side detectors, positioned at polar angles of 24.5 $^\circ$ and azimuthal angles 0 $^\circ$, 90 $^\circ$, 180 $^\circ$, and 270 $^\circ$ (labelled L, U, R, D), and the forward detector (labelled F). Figure 1 shows the deviation of the measured ratios $r^{Cx}(E_c)$ and the quadratic fits $r_{fit}^{Cx}(E_c)$ from the fit r_{fit}^{Au5} to the reference data $r^{Au}(E_c)$. The figure corresponds to figure 2 of reference [3] for the linear fits. From the $r_{fit}^{Cx}(E_c)$ and
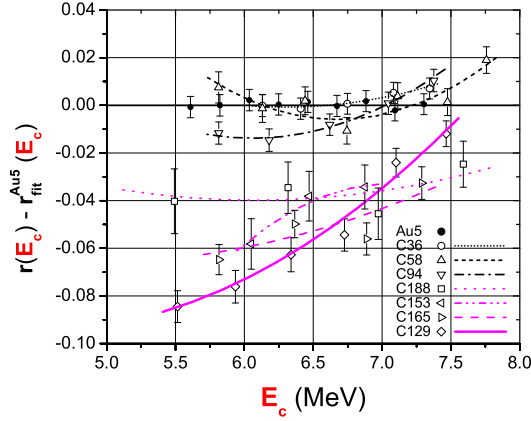
Figure 1. Difference between the fits and measured ratios $r(E_c)$ and the fit to the Au5 data. To ease readability, data points were combined. The fit lines cover the full energy ranges given in table 1. The given errors include the statistical errors of the measured ratios and the sample standard deviation [5] of the fit to the Au5 ratios.

$r_{\mathrm{fit}}^{\mathrm{Au5}}(E_c)$ the following expression for p_{zz} of the beam is obtained [3],

$$p_{zz}^{\mathrm{Cx}}(E_c) = \frac{2 \cdot [r_{\mathrm{fit}}^{\mathrm{Au5}}(E_c) - r_{\mathrm{fit}}^{\mathrm{Cx}}(E_c)]}{r_{\mathrm{fit}}^{\mathrm{Cx}}(E_c)A_{zz}(E_c, 0\,^\circ) - r_{\mathrm{fit}}^{\mathrm{Au5}}(E_c)A_{zz}(E_c, 24.5\,^\circ)} \,. \tag{4}$$

It is obvious from equation 2 that, for two targets of different thickness but identical E_c, the difference in p_{zz} has to be attributed to the additional range of higher deuteron energy in the thicker target. Therefore, in figure 2 the seven sets of p_{zz} are plotted as a function of the initial
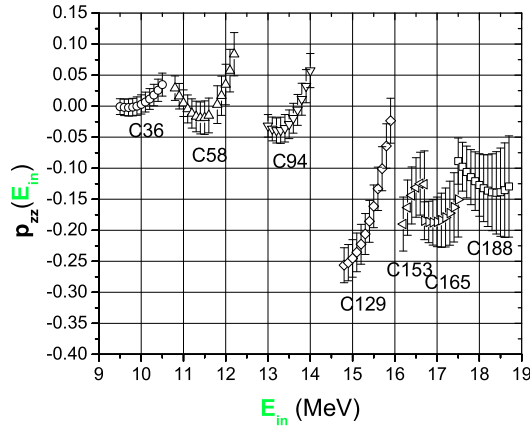

Figure 2. Deuteron tensor polarization p_{zz} produced in the seven carbon targets as a function of initial beam energies E_{in}. The errors include those caused by uncertainties of the target thickness.
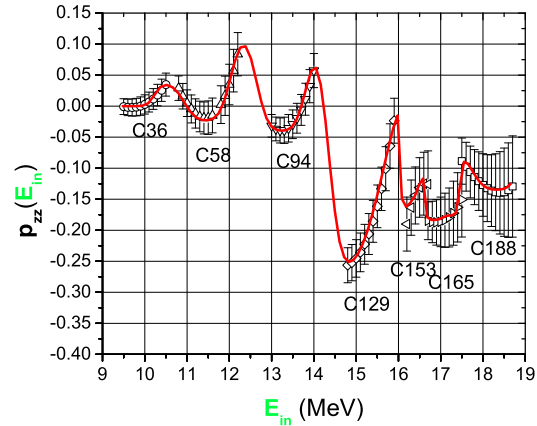
Figure 3. The p_{zz} distribution of figure 2 and the distribution calculated with 15 Gaussian-distributed cross sections describing the deuteron-carbon interaction in equation 2.

beam energy E_{in}. The coarse structure of the energy dependence corresonds to that derived with the linear fit functions ([3], figure 3), whereas the energy dependence within the data sets for the individual targets are modified by the use of the quadratic fit functions. The deviation from the calculated [4] smooth energy dependence is more pronounced than that resulting from the linear fit functions (cf. figure 3 of reference [3]).

To describe the production of polarization during deceleration in the targets with the use of equation 2, the energy dependences of the cross sections $\sigma_{\pm 1}(E)$ and $\sigma_0(E)$ are assumed to be

Gaussian-distributed,

$$\sigma_{\pm 1,0}(E) = \sigma_{\pm 1,0}(E_0) \cdot e^{-2.7707 \cdot (\frac{E-E_0}{\Gamma_{1/2}})^2} . \tag{5}$$

The integrals of equation 2 are replaced by sums over thin target layers, the deuteron energy $E(x)$ within each layer is calculated with the use of the Bethe-Bloch energy-loss formula. The parameters $\sigma_{\pm 1,0}(E_0)$, E_0 and $\Gamma_{1/2}$ were varied in a manual procedure to reproduce the measured energy dependence. Either $\sigma_{\pm 1}(E_0) > 0$, $\sigma_0(E_0) = 0$, resulting in $p_{zz} < 0$, or $\sigma_{\pm 1}(E_0) = 0$, $\sigma_0(E_0) > 0$, resulting in $p_{zz} > 0$, were chosen to reproduce the slope in the energy dependence. The parameters of the 15 cross-section distributions, requested for a reasonable fit (figure 3), are given in table 2. Unfortunately, the present measurements do not cover the range between E_{in}=14.0 and 14.8 MeV. The distinct jump in p_{zz} requests the peak no. 10 around E_0=14.4 MeV. The estimated errors of the data given in table 2, are $\leq$0.3 MeV for E_0 and $E^*(^{14}N)$, $\leq$ 20% for $\Gamma_{1/2}$, and 10 to 20% for p_{zz}.

Table 2. The parameters E_0, $\sigma(E_0)$, and $\Gamma_{1/2}$ of the cross-section distributions describing the deuteron-carbon interaction, the tensor polarization p_{zz} produced by the single peak, and the excitation energy in the compound nucleus ^{14}N at the laboratory energy E_0 (error estimates are given in the text).

no.	E_0 [MeV]	$\sigma(E_0)$ [b]	$\Gamma_{1/2}$ [keV]	p_{zz}	$E^*(^{14}N)$ [MeV]
1	19.0	300	500	0.13	26.5
2	17.8	150	500	−0.06	25.5
3	17.5	860	150	0.10	25.3
4	17.1	50	200	0.01	24.9
5	16.7	1050	80	−0.07	24.6
6	16.5	240	200	0.04	24.4
7	16.1	2300	100	−0.18	24.1
8	15.9	140	500	0.05	23.9
9	15.6	380	900	0.24	23.6
10	14.4	1100	520	−0.39	22.6
11	13.9	500	500	0.16	22.2
12	12.7	530	500	−0.16	21.1
13	12.1	500	500	0.15	20.6
14	11.0	220	500	−0.06	19.7
15	10.3	220	320	0.04	19.1

The excitation energies in the compound nucleus $E^*(^{14}N)$, calculated from the d, ^{12}C, ^{14}N masses and the laboratory energy E_0, are in surprising agreement with the energies of known ^{14}N states [6]. This finding indicates resonance formation of compound states in the d-^{12}C interaction at appropriate deuteron energies during deceleration in the targets. A similar interpretation has been given for the measured selective structure of the excitation function in elastic d-^{12}C scattering [7] at lower deuteron energies. The present data for the cross sections at E_0=14.4 and 15.6 MeV reflect the structure in the excitation function of the reaction $^{12}C(d,\alpha)^{10}B^*(1.74 MeV)$ [6]. These similarities may lead the way to interpret the present results.

The relative differences of proton-count numbers in the side detectors can be used to investigate the azimuthal property of the beam behind the targets. The figure 4 shows the average values of the ratios $(N_L - N_R)/(N_L + N_R)$ and $(N_U - N_D)/(N_U + N_D)$ for the seven graphite targets. The values are corrected for the count ratios, measured with the gold target, to take into account diffrences in the counting efficiencies. All values are compatibal with zero and the fact that the vector polarization in the beams behind the spin-zero carbon targets has to be zero.

3. The possibility to produce tensor polarized deuteron beams
The present data, especially those of the deuteron-energy range around 15 MeV, indicate the possibility to produce tensor polarized deuteron beams by passing initially unpolarized deuteron beams through targets made from graphite. The expected polarization can be calculated with the use of the peak parameters of table 2 and the equation 2. The figure 5 shows the results for
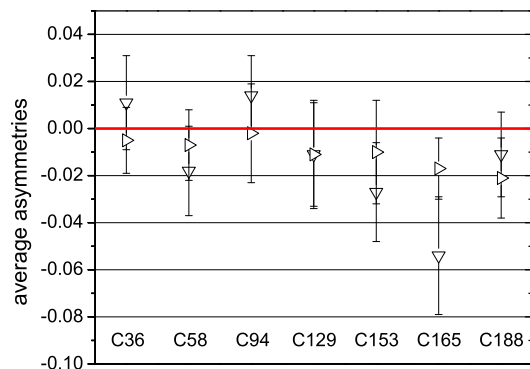
Figure 4. The average asymmetries $(N_{\mathrm{L}} - N_{\mathrm{R}})/(N_{\mathrm{L}} + N_{\mathrm{R}})$ (triangleright) and $(N_{\mathrm{U}} - N_{\mathrm{D}})/(N_{\mathrm{U}} + N_{\mathrm{D}})$ (triangledown), measured with the seven graphite targets and corrected for that measured with the gold target.

initial beam energies of 14.8 and 15.8 MeV. In deceleration from 14.8 to $\sim$14 MeV the deuterons pass the energy range, where the cross section is described by the peak around 14.4 MeV with $\sigma_{\pm1}(E) > 0$ and $\sigma_0(E) = 0$. A p_{zz} of about -0.3 and E_{out}=14 MeV result behind a 20 mg/cm^2 carbon target. The polarization is maintained for thicker targets, allowing the choice of lower values of E_{out}. For E_{in}=15.8 MeV, a 20 mg/cm^2 target with E_{out}=14.8 MeV yields p_{zz} of about +0.2 due to the effect by the peak around 15.4 MeV ($\sigma_{\pm1}(E) = 0$ and $\sigma_0(E) > 0$). For thicker targets and lower values of E_{out}, p_{zz} of about -0.1 would result due to the effect by the peak around 14.4 MeV. With the use of a sandwiched material, causing deceleration from 14.8 to 14 MeV without polarizing effects, the positive p_{zz} could be maintained also for thicker targets and lower values of E_{out}.
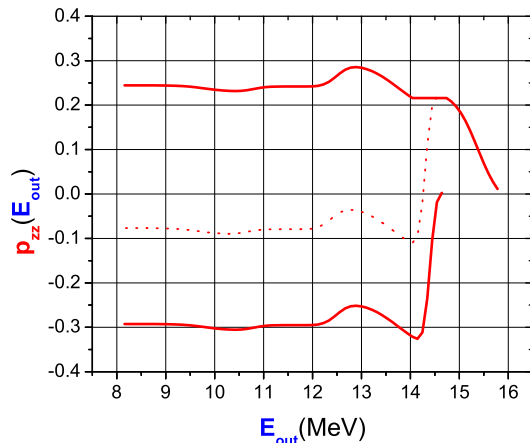

Figure 5. Tensor polarization p_{zz} produced by graphite targets from unpolarized deuteron beams as function of the energy behind the target, E_{out}, depending on the target thickness (lower full line: E_{in}=14.8 MeV; upper lines (E_{in}=15.8 MeV): the full line for a target with a different sandwiched material suppressing the negative polarization by carbon around 14.4 MeV, the dotted line below E_{out}=14.8 MeV for a pure graphite target.

4. Conclusion and outlook

Contrary to the earlier analysis with linear functions, in the present work the measured count-number ratios were fitted by quadratic fit functions (figure 1). The present distribution of the tensor polarization p_{zz} of the deuteron beam behind the graphite targets as function of the initial beam energy (figure 2) differs slightly from that obtained with linear fit functions (figure 3 in reference [3]). The fit of the present p_{zz} distribution (figure 3) among the fit parameters of table 2 yields central energies E_0 slightly differing from those given in reference [3]. The essential structure of the energy dependence, however, is the same. Unfortunately, no measurements have been performed to fill the gaps of initial beam energies from 12.2 to 13.0 MeV and from 14.0 to 14.8 MeV. The setup at Universität zu Köln, used in the present measurements, meanwhile has been disassembled. It would be desirable to continue the measurements at another facility to

confirm and to complete the present results.

[a] present address AREVA NP GmbH, 91058 Erlangen, Germany
[b] present address TU München, Physics Department E18, 85748 Garching, Germany
[c] present address Brookhaven National Laboratory, Upton, NY 11973, USA

References

[1] Baryshevsky V G 1992 *Phys. Lett* A **171** 431
[2] Haeberli W 1967 *Ann. Rev. Nucl. Sci.* **17** 373
[3] Seyfarth H et al 2010 *Phys. Rev. Lett.* **104** 222501
[4] Baryshevsky V and Rouba A 2010 *Phys. Lett.* B **683** 229
[5] Bevington P R 1969 *Data Reduction and Error Analysis for the Physical Sciences* (New York: McGraw Hill)
[6] Ajzenberg-Selove F 1991 *Nucl. Phys.* A **523** 1
[7] Ohlsen G G and Shamu R E 1963 *Nucl. Phys.* **45** 523